

# Implant Isolation of Silicon Two-Dimensional Electron Gases at 4.2 K

Chiao-Ti Huang, Jiun-Yun Li, and James C. Sturm, *Fellow, IEEE*

**Abstract**—Successful lateral electrical isolation of silicon 2-D electron gases (2DEGs) at liquid helium temperature (4.2 K) by ion implantation is demonstrated. The sheet resistance of the implanted regions can be achieved as high as  $1 \times 10^{13} \Omega/\square$  at 4.2 K. Thermal stability up to 550 °C makes the technique compatible with most subsequent processing steps to fabricate silicon quantum devices. It has also been confirmed that the 2DEG quality is not degraded by the ion implantation, based on a comparison of Hall mobility of implant-isolated samples with conventional reactive-ion-etching-defined samples.

**Index Terms**—Ion implantation, isolation, Si/SiGe heterostructure, 2-D electron gas (2DEG).

## I. INTRODUCTION

SINGLE-electron quantum-dot devices based on the Si/SiGe material system are attractive for quantum computation due to the weak spin-orbit coupling in silicon and resulting longer spin coherence time [1], [2]. Such quantum devices are typically fabricated in modulation-doped (depletion-mode) or undoped (enhancement-mode) 2-D electron gases (2DEGs) [3]–[5]. 2DEGs are usually electrically isolated by mesa etching. However, the mesa edges can cause problems for subsequent fabrication steps, such as the application of electron-beam resist for submicrometer gates to form quantum dots and thin metal step coverage. In addition, in enhancement-mode devices, high electrical fields in the gate insulator above the corner of the etched mesa may cause breakdown of the insulator or leakage currents.

Ion implantation for lateral electrical isolation (“implant isolation”) on III–V materials has been a well-known technique for several decades [6]. Ion bombardment creates deep defect levels, and these defects trap free electrons and pin Fermi level near midgap, resulting in high resistivity. This process not only provides excellent electrical isolation but also preserves the planarity of the surface. However, relatively few papers have focused on implant isolation in Si-based devices [7], because the resulting high-resistivity regions cannot sustain post-isolation high-temperature processes ( $> 1000$  °C) common in silicon

Manuscript received October 8, 2012; revised October 25, 2012; accepted November 4, 2012. Date of publication December 13, 2012; date of current version December 19, 2012. This work was supported in part by the Defense Advanced Research Projects Agency under Grant HR0011-09-1-0007, by the Army Research Office under Grant W911NF-09-1-0498, and by the National Science Foundation MRSEC Program through the Princeton Center for Complex Materials under Grant DMR-0819860. The review of this letter was arranged by Editor E. A. Gutiérrez-D.

The authors are with the Princeton Institute for the Science and Technology of Materials, Department of Electrical Engineering, Princeton University, Princeton, NJ 08544 USA (e-mail: chiaoti@princeton.edu).

Digital Object Identifier 10.1109/LED.2012.2228160

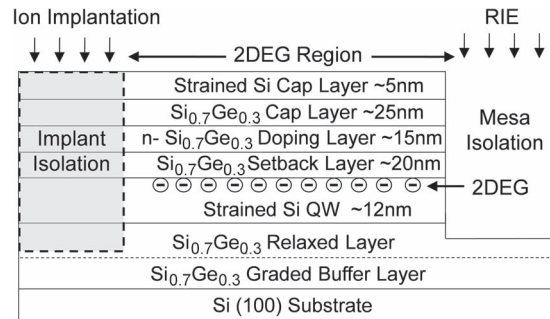


Fig. 1. Layer structure of a test sample. The layers above the horizontal dotted line were grown by RTCVD. To pattern the 2DEG, only one of implant isolation or conventional mesa isolation by RIE is used on a single sample, but both are illustrated in this figure for brevity.

technology. Furthermore, the resistivity of the intrinsic silicon (Fermi level at midgap) is  $\sim 2 \times 10^5 \Omega \cdot \text{cm}$  at room temperature, which is not high enough for most applications. However, the processing of Si/SiGe-based quantum devices is often constrained to be below 600 °C to avoid Si/Ge interdiffusion [8], which could be low enough to avoid annealing of implant damage. Moreover, the typical low operation temperature (4.2 K or less) of such quantum devices provides much less thermal energy for electrons to escape from implant-induced defects, so that resistivities much higher than those in silicon at room temperature should be possible.

In this letter, we demonstrate implant isolation of modulation-doped Si 2DEG structures characterized at 4.2 K. Heavily doped 2DEGs were used to examine the isolation capability as a worst case (high electron density of  $\sim 10^{12} \text{ cm}^{-2}$ ). The thermal stability was tested for different post-implant annealing temperatures up to 650 °C. The 2DEG quality (electron mobility) of samples processed with implant isolation was compared with the ones with conventional mesa isolation by reactive ion etching (RIE).

## II. SAMPLE GROWTH AND FABRICATION

The layer structure of the modulation-doped Si 2DEGs used in this study is shown in Fig. 1. Their Hall mobility, electron density, and sheet resistance at 4.2 K are in the range of 80 000–150 000  $\text{cm}^2/\text{V} \cdot \text{s}$ ,  $0.8\text{--}1.6 \times 10^{12} \text{ cm}^{-2}$ , and  $30\text{--}80 \Omega/\square$ , respectively. The structures were all grown on  $\text{Si}_{0.7}\text{Ge}_{0.3}$  graded buffer substrates by rapid thermal chemical vapor deposition (RTCVD) between 575 °C and 625 °C. A test device consists of a set of separated ohmic contacts to test the implant isolation and a Hall bar structure (in a single 2DEG region) with ohmic contacts to measure electron mobility and

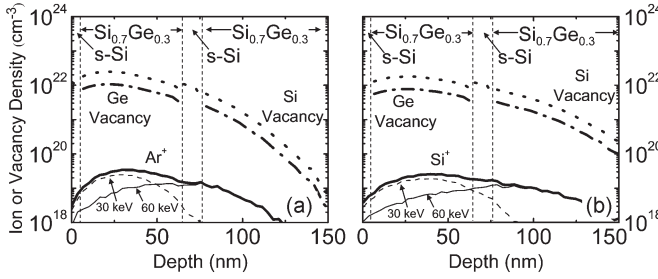


Fig. 2. Simulation of implanted species and resulting vacancy distribution in a 2DEG structure by the stopping and range of ions in matters software [10]. Two-step implantation ( $1 \times 10^{14} \text{ cm}^{-2}$  at 30 keV +  $1 \times 10^{14} \text{ cm}^{-2}$  at 60 keV) with implanted species (a)  $\text{Ar}^+$  and (b)  $\text{Si}^+$  is used in this simulation. The target is assumed to be implanted at 0 K.

density. After 2DEG growth, a 400-nm screen silicon dioxide layer was first deposited by plasma-enhanced chemical vapor deposition at 250 °C. Ohmic contact regions to the 2DEG were then defined by photolithography and diluted HF wet etching of the oxide. One-percent Sb-doped Au was thermally evaporated followed by lift-off. Annealing at 450 °C for 10 min to form ohmic alloyed contacts was performed before the ion implantation except for samples later annealed at 550 °C or 650 °C, where the contacts were formed after 550 °C or 650 °C steps. The areas to be isolated were then defined by photolithography and diluted HF wet etching of the oxide.

Isolation tests were done by implanting separately argon ( $\text{Ar}^+$ ) and silicon ( $\text{Si}^+$ ) ions into different samples. Si and Ar were chosen due to their electrical neutrality in the Si/SiGe material system. Two implant energies were used in all regions because both the 2DEG channel and the doping supply layer (if doped above the metal–insulator transition level) [9] could conduct electricity at low temperature. Therefore, two ion implantation energies of 30 and 60 keV were used to create defects near the depth of the shallow doping supply layer (30 keV) and near the deeper strained Si 2DEG channel (60 keV), respectively (Fig. 2). Silicon amorphized by a high-dose implant ( $\sim 5 \times 10^{14} \text{ cm}^{-2}$  for  $\text{Si}^+$  into Si at 40 keV) [11] can be recrystallized by solid-phase epitaxy (SPE) at a temperature of as low as 500 °C [12] (which would lead to poor thermal stability of the damage). Further, SiGe alloys are even more easily amorphized by ion implantation than Si due to weaker bonding between Si and Ge atoms [13]. Therefore, doses well below  $5 \times 10^{14} \text{ cm}^{-2}$  were used.  $\text{Ar}^+$  or  $\text{Si}^+$  was then implanted at room temperature with three different test doses:  $5 \times 10^{11} \text{ cm}^{-2}$  (denoted as low dose),  $1 \times 10^{13} \text{ cm}^{-2}$  (medium dose), and  $1 \times 10^{14} \text{ cm}^{-2}$  (high dose), and each dose was implanted at two energies, 30 and 60 keV. In addition, Hall bars defined by conventional mesa isolation by RIE were also made for 2DEG quality comparison. Ohmic contacts were made on one  $\text{Si}_{0.7}\text{Ge}_{0.3}$  graded buffer substrate separately without implant isolation to test its resistivity at 4.2 K for reference.

### III. RESULTS AND DISCUSSION

The isolation capability at 4.2 K was examined by two-point measurements between two implant-isolated 2DEGs. The sheet resistances of isolated regions for all six implant conditions

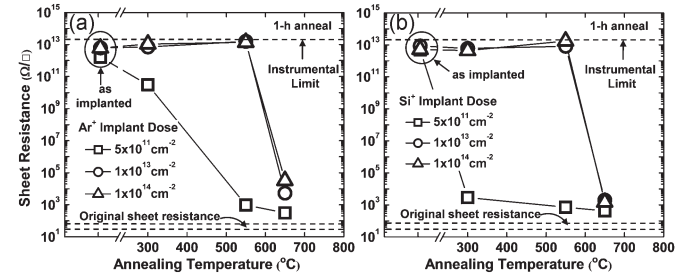


Fig. 3. Isochronal (1-h) annealing behavior of sheet resistances of 2DEG samples at 4.2 K implanted with (a)  $\text{Ar}^+$  and (b)  $\text{Si}^+$  with three various doses,  $5 \times 10^{11} \text{ cm}^{-2}$ ,  $1 \times 10^{13} \text{ cm}^{-2}$  and  $1 \times 10^{14} \text{ cm}^{-2}$  at 30 and 60 keV. Also shown are the range of sheet resistance of the starting 2DEGs and the experimental instrumental limitation. The estimated error of sheet resistance is  $\pm 18\%$  for (a) and  $27\%$  for (b).

are all above  $1 \times 10^{12} \Omega/\square$ , which is ten orders of magnitude higher than the original 2DEG sheet resistances (Fig. 3). In some cases, the sheet resistance is as high as  $1 \times 10^{13} \Omega/\square$ , close to the instrumental limit. Since the sheet resistance of the  $\text{Si}_{0.7}\text{Ge}_{0.3}$  graded buffer substrate at 4.2 K was also high ( $\sim 5 \times 10^{12} \Omega/\square$ ), the remaining conduction might occur either in the relaxed SiGe buffer or in the implanted regions. In any case, it is clear that the implant isolation for all three doses is extremely effective.

Thermal stability issues could arise when we integrate implant isolation technique into a device fabrication process, for example, insulator deposition and contact annealing. Aluminum oxide deposited by atomic layer deposition is a common insulator used on enhancement-mode Si 2DEG devices due to its high quality and low deposition temperature ( $\leq 300$  °C) [14]. To test the thermal stability at the oxide deposition temperature, samples were annealed at 300 °C for 1 h, and their sheet resistances were measured at 4.2 K (Fig. 3). For samples implanted with medium and high doses, the sheet resistances stay high at  $\sim 1 \times 10^{13} \Omega/\square$  regardless of implant species, while for ones implanted with a low dose, the sheet resistances drop to  $3 \times 10^{10} \Omega/\square$  and  $3 \times 10^3 \Omega/\square$  for  $\text{Ar}^+$  and  $\text{Si}^+$  implants, respectively. Since implantation with the lowest dose ( $1 \times 10^{11} \text{ cm}^{-2}$ ) produces the fewest defects (mostly point defects), the damage is easy to be annealed, and thus, the sheet resistance decreases. In addition, the higher sheet resistance of low-dose  $\text{Ar}^+$ -implanted sample than  $\text{Si}^+$ -implanted one after 300 °C annealing might be explained by a higher damage level caused by  $\text{Ar}^+$  due to its heavier atomic mass.

Antimony-doped gold is commonly used on both depletion-mode and enhancement-mode Si/SiGe devices to form ohmic alloyed contacts after annealing [14]. However, the necessity of an overlap between the insulated gate and contacts in the enhancement-mode devices for the continuity of conduction makes the requirement of a flat contact surface crucial to prevent possible leakage. Because alloyed contacts have rough surfaces, contacts made by n-type ion implantation are preferred [4], [5]. For heavily phosphorus-implanted contacts, the activation of implanted phosphorus occurs at relatively low temperature ( $\geq 500$  °C) by SPE [12]. Hence, the thermal stability of implant isolation samples was again tested after 550 °C annealing for 1 h. Sheet resistances of the medium- and high-dose samples at 4.2 K are still as high as  $1 \times 10^{13} \Omega/\square$  (Fig. 3).

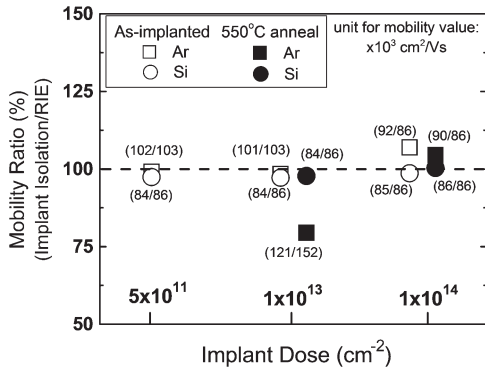


Fig. 4. Comparison of 2DEG quality after implant isolation or RIE process by the ratio of the mobility at 4.2 K measured from an implant-isolation-defined Hall bar to a RIE-defined Hall bar for a given implant and anneal. The absolute mobility values at 4.2 K with a unit of  $10^3 \text{ cm}^2/\text{Vs}$  are shown in parentheses with the mobility for implant isolation before the mobility for mesa isolation. The estimated error of mobility measurement is  $\pm 5\%$ .

After further annealing at  $650^\circ\text{C}$  for 1 h, the sheet resistances of the medium- and high-dose samples at 4.2 K drop nine orders of magnitude. Therefore, if an annealing temperature for the contact over  $550^\circ\text{C}$  is desired, it should be done before implant isolation.

Any possible degradation of the 2DEG quality due to spurious radiation during ion implantation was investigated based on Hall mobility measurement by standard low-frequency lock-in techniques at 4.2 K. Fig. 4 shows the ratio of mobility measured from implant-isolation-defined Hall bars to RIE-defined ones (with absolute mobility values shown in parentheses) from the same CVD growth and annealing condition. Implanted samples without annealing (open symbols) do not show any significant mobility degradation. Even with the highest dose used in this study ( $1 \times 10^{14} \text{ cm}^{-2}$ ), the 2DEG quality remains unaffected. Mobility ratios of samples experiencing both implant isolation and  $550^\circ\text{C}$  annealing are also shown in Fig. 4 (closed symbols). Except for one sample, the mobility ratios after  $550^\circ\text{C}$  annealing are near 100%. We attribute the low mobility ratio for the medium-dose  $\text{Ar}^+$ -implanted sample to a nonuniformity in the 2DEG growth between different wafer pieces used for the Hall bars.

#### IV. SUMMARY AND CONCLUSION

Excellent electrical isolation of silicon 2DEGs by ion implantation has been demonstrated. A sheet resistance of implanted regions as high as  $1 \times 10^{13} \Omega/\square$  at 4.2 K is achieved. Samples implanted by  $\text{Ar}^+$  and  $\text{Si}^+$  at medium

( $1 \times 10^{13} \text{ cm}^{-2}$ ) and high doses ( $1 \times 10^{14} \text{ cm}^{-2}$ ) present excellent thermal stability even after  $550^\circ\text{C}$  annealing. No degradation of the 2DEG was observed due to the isolation implant.

#### ACKNOWLEDGMENT

The authors would like to thank Amberwave semiconductor for providing the relaxed SiGe buffers on silicon and J. Petta of Princeton for stimulating discussions.

#### REFERENCES

- [1] R. Hanson, L. P. Kouwenhoven, J. R. Petta, S. Tarucha, and L. M. K. Vandersypen, "Spins in few-electron quantum dots," *Rev. Mod. Phys.*, vol. 79, no. 4, pp. 1217–1265, Oct. 2007.
- [2] A. M. Tyryshkin, S. A. Lyon, A. V. Astashkin, and A. M. Raitsimring, "Electron spin relaxation times of phosphorus donors in silicon," *Phys. Rev. B*, vol. 68, no. 19, pp. 193207-1–193207-4, Nov. 2003.
- [3] T. Berer, D. Pachinger, G. Pillwein, M. Muhlberger, H. Lichtenberger, G. Brunthaler, and F. Schaffler, "Lateral quantum dots in Si/SiGe realized by a Schottky split-gate technique," *Appl. Phys. Lett.*, vol. 88, no. 16, pp. 162112-1–162112-3, Apr. 2006.
- [4] T. M. Lu, N. C. Bishop, T. Pluym, J. Means, P. G. Kotula, J. Cederberg, L. A. Tracy, J. Dominguez, M. P. Lilly, and M. S. Carroll, "Enhancement-mode buried strained silicon channel quantum dot with tunable lateral geometry," *Appl. Phys. Lett.*, vol. 99, no. 4, pp. 043101-1–043101-3, Jul. 2011.
- [5] B. M. Maune, M. G. Borselli, B. Huang, T. D. Ladd, P. W. Deelman, K. S. Holabird, A. A. Kislev, I. Alvarado-Rodriguez, R. S. Ross, A. E. Schmitz, M. Sokolich, C. A. Watson, M. F. Gyure, and A. T. Hunter, "Coherent singlet-triplet oscillations in a silicon-based double quantum dot," *Nature*, vol. 481, no. 7381, pp. 344–347, Jan. 2012.
- [6] S. J. Pearton, "Ion implantation for isolation of III-V semiconductors," *Mater. Sci. Rep.*, vol. 4, no. 6, pp. 313–363, Oct. 1989.
- [7] J. A. Yasaitis, "Ion implantation of neon in silicon for planar amorphous isolation," *Electron. Lett.*, vol. 14, no. 15, pp. 460–462, Jul. 1978.
- [8] T. M. Lu, N. C. Bishop, T. Pluym, J. Dominguez, J. E. Bower, J. Cederberg, P. G. Kotula, L. A. Tracy, J. Means, M. P. Lilly, and M. S. Carroll, "Process development toward enhancement-mode strained-Si/SiGe double quantum dot," in *Proc. ISTDM*, 2012, pp. 1–2.
- [9] C. Yamanouchi, K. Mizuguchi, and W. Sasaki, "Electric conduction in phosphorus doped silicon at low temperature," *J. Phys. Soc. Jpn.*, vol. 22, no. 3, pp. 859–864, Mar. 1967.
- [10] J. F. Ziegler, J. P. Biersack, and L. Haggmark, (2012), *The Stopping and Ranges of Ions in Matter*. [Online]. Available: [www.srim.org](http://www.srim.org)
- [11] J. F. Gibbons, "Ion implantation in semiconductors—Part II: Damage production and annealing," *Proc. IEEE*, vol. 60, no. 9, pp. 1062–1096, Sep. 1972.
- [12] S. A. Campbell, *Fabrication Engineering at the Micro- and Nanoscale*, 3rd ed. New York: Oxford Univ. Press, 2008, pp. 124–125.
- [13] A. N. Larsen, C. ORaifeartaigh, R. C. Barklie, B. Holm, F. Priolo, G. Franzo, G. Lulli, M. Bianconi, R. Nipoti, J. K. N. Lindner, A. Mesli, J. J. Grob, F. Cristiano, and P. L. F. Hemment, "MeV ion implantation induced damage in relaxed  $\text{Si}_{1-x}\text{Ge}_x$ ," *J. Appl. Phys.*, vol. 81, no. 5, pp. 2208–2218, Mar. 1997.
- [14] T. M. Lu, D. C. Tsui, C.-H. Lee, and C. W. Liu, "Observation of two-dimensional electron gas in a Si quantum well with mobility of  $1.6 \times 10^6 \text{ cm}^2/\text{Vs}$ ," *Appl. Phys. Lett.*, vol. 94, no. 18, pp. 182102-1–182102-3, May 2009.